UDK 539.3:534.242

O. P. Piddubniak, N. G. Piddubniak

SOUND RADIATION FROM VEHICLES ON THE RIGHT-ANGLE BEND IN THE ROAD

Sound radiation from vehicles traveling on a city road with a right-angle bend is studied. The effect of wind on the acoustic field is taken into account. First, a solution to the problem for two-point noise sources moving in opposite directions is found using the integral Fourier transforms over space variables and time. Inverse transforms are calculated approximately using the stationary phase method. A solution to the general problem is obtained as a superposition of many partial solutions. The numerical analysis of traffic noise characteristics is carried out for the case of a dual carriageway Textile Workers Avenue in the town of Łódź, Poland.

Introduction. A bend in the road is one of many elements of city streets. Because of a change in the direction of car motion, this element is an important source of noise. Noise generated at a street bend must be different from the noise generated by cars traveling on a straight road. However, theoretical investigations on this field of acoustic environment have not been sufficiently developed yet.

Recently, Chevallier et al. [3] proposed a model of noise propagation from a roundabout. In this work, the state of theoretical and experimental researches on traffic noise generated near a roundabout were presented. At the same time, however in a different way, we investigated noise propagation from vehicles traveling at a roundabout taking into account wind and sound wave reflection from an elastic half-space [9]. It was found that the roundabout is a place of a significant sound concentration. Therefore, such behavior must be expected also in the case of a road with unclosed arc form [16]. In our new model, we also take into account the two-way traffic of transport vehicles. In real conditions, the inhomogeneity, temperature and humidity of air, as well as the state of roadbed and traffic composition, have an essential influence on the formation of sound field structure [7, 13, 14]. Therefore, this problem is very complicated. In previous studies [10, 12], considering the mathematical model of acoustic waves generated from the straight section of a city multi-carriageway road and from a traffic crossroad, we showed that the structure of traffic noise strongly depended on the type of vehicles, their velocities and frequency of sound emission from single sources, the road geometry, as well as the velocity and direction of wind.

The main goal of this work is to formulate and numerically implement an analytical algorithm for the analysis of acoustic pressure and power flow density caused by many vehicles moving in two mutually opposite directions on a city dual carriageway road consisting of six lanes with a right-angle bend in windy conditions.

1. Formulation of the problem and the method for its solution. Let us consider the problem of sound propagation from vehicles traveling in a road with a right-angle bend of radius $\xi = \xi_0$ and angular coordinate θ, $3\pi/2 \le \theta \le 2\pi$. Two types of vehicles are involved in this study, namely, personal cars (L) and heavy trucks (C). They travel at constant velocities v_{L} and v_{C}, respectively. The intervals between discrete vehicles are Δ_{L} and Δ_{C}. The road has six lanes with two, anticlockwise and clockwise, directions of motion for personal cars and heavy trucks on quarter circles with radii $\xi = \xi_0 \pm \xi_{\mathrm{L}1}$, $\xi = \xi_0 \pm \xi_{\mathrm{L}2}$ and $\xi = \xi_0 \pm \xi_{\mathrm{C}}$, $\xi_{\mathrm{L}1} < \xi_{0,}$, $\xi_{\mathrm{L}2} < \xi_{0,}$, $\xi_{\mathrm{C}} < \xi_0$. The vehicles, as the carriers of noise, are determined by point sources located at constant heights $z = h_{\mathrm{L}}$ and $z = h_{\mathrm{C}}$, $h_{\mathrm{L}} < h_{\mathrm{C}}$, with force vector intensities $\mathbf{F}_{\mathrm{L}}$

and $\mathbf{F}_C$ and with sound radiation frequencies Ω_L and Ω_C. Assume that an acoustic medium moves parallel to the road plane at constant velocity vector $\mathbf{v}_w = (v_{wx}, v_{wy}, 0)$ in direction θ_w to axis Ox, where $v_{wx} = v_w \cos\theta_w$, $v_{wy} = v_w \sin\theta_w$ and $v_w = |\mathbf{v}_w|$.

The basic relations for linear acoustics of the moving media are the equation of motion and mass balance equation [8]:

$$\rho \frac{d\mathbf{v}(\mathbf{x},t)}{dt} = -\nabla p(\mathbf{x},t) + \mathbf{F}(\mathbf{x},t), \tag{1}$$

$$\nabla \cdot \mathbf{v}(\mathbf{x},t) = -\frac{1}{\rho c^2}\frac{dp(\mathbf{x},t)}{dt}, \tag{2}$$

where $p(\mathbf{x},t)$ is the acoustic pressure, $\mathbf{v}(\mathbf{x},t)$ is the particle velocity, ρ is the acoustic density, c is the sound velocity, t is the time, ∇ is the Hamilton operator, $\nabla = \nabla_\perp + \mathbf{i}_z \partial/\partial z$, where $\nabla_\perp = \mathbf{i}_x \partial/\partial x + \mathbf{i}_y \partial/\partial y$, $\mathbf{i}_x$, $\mathbf{i}_y$, $\mathbf{i}_z$ are the unit vectors. The full derivative with respect to time is determined as $d/dt \equiv \partial/\partial t + \mathbf{v}_w \cdot \nabla_\perp$. Note that the particle velocity vector is connected with particle displacement vector in moving acoustic medium by the relation

$$\mathbf{v}(\mathbf{x},t) = \frac{d\mathbf{u}(\mathbf{x},t)}{dt} = \frac{\partial \mathbf{u}(\mathbf{x},t)}{\partial t} + \mathbf{v}_w \cdot \nabla_\perp \mathbf{u}(\mathbf{x},t). \tag{3}$$

In (1), $\mathbf{F}(\mathbf{x},t)$ is the complex mass load vector, $\mathbf{F}(\mathbf{x},t) = \mathbf{F}_0 G(\boldsymbol{\xi},t)\delta(z - z_0)$, where $\mathbf{F}_0$ is the vector of constant mass load real amplitudes, $\delta(z)$ is the Dirac function, $G(\boldsymbol{\xi},t)$ is the function characterizing complex mass load distribution in plane Oxy; $\mathbf{x} = \boldsymbol{\xi} + \mathbf{i}_z z$ and $\boldsymbol{\xi} = \mathbf{i}_x x + \mathbf{i}_y y$ are the radius-vectors in space $Oxyz$ and in plane Oxy, respectively.

On the acoustic medium – elastic half-space interface $(z = 0)$, the following conditions should be satisfied:

$$\sigma_z + p_{tot} = 0, \quad \tau_{xz} = 0, \quad \tau_{yz} = 0, \quad u_{sz} = u_{tot,z}, \tag{4}$$

where $p_{tot} = p_{rad} + p_{ref}$, $u_{tot,z} = u_{rad,z} + u_{ref,z}$ are the total acoustic pressure and total normal component of particle displacement vector in acoustic medium $z > 0$, respectively, σ_z, τ_{xz} and τ_{yz} are the stress tensor components in the elastic half-space $z < 0$, and u_{sz} is the component of elastic displacement vector. The «rad» and «ref» indices denote the waves radiated by a sound source and reflected from plane $z = 0$ in the acoustic medium. The source term in (1) for the reflected wave may be neglected.

Elastic stress tensor $\boldsymbol{\sigma}(\mathbf{x},t)$ and displacement vector $\mathbf{u}_s(\mathbf{x},t)$ are expressed by the following relations [2]:

$$\sigma_z(\mathbf{x},t) = \lambda \nabla^2 \varphi(\mathbf{x},t) + 2\mu \left\{ \frac{\partial^2 \varphi(\mathbf{x},t)}{\partial z^2} + \frac{\partial}{\partial z}\left[\frac{\partial \psi_y(\mathbf{x},t)}{\partial x} - \frac{\partial \psi_x(\mathbf{x},t)}{\partial y} \right] \right\}, \tag{5}$$

$$\tau_{xz}(\mathbf{x},t) = \mu \left[2\frac{\partial^2 \varphi(\mathbf{x},t)}{\partial x \partial z} - 2\frac{\partial^2 \psi_x(\mathbf{x},t)}{\partial x \partial y} + \left(\frac{\partial^2}{\partial x^2} - \frac{\partial^2}{\partial y^2} - \frac{\partial^2}{\partial z^2} \right) \psi_y(\mathbf{x},t) \right], \tag{6}$$

$$\tau_{yz}(\mathbf{x},t) = \mu \left[2\frac{\partial^2 \varphi(\mathbf{x},t)}{\partial y \partial z} + \left(\frac{\partial^2}{\partial x^2} - \frac{\partial^2}{\partial y^2} + \frac{\partial^2}{\partial z^2} \right) \psi_x(\mathbf{x},t) + 2\frac{\partial^2 \psi_y(\mathbf{x},t)}{\partial x \partial y} \right], \tag{7}$$

$$u_{sz}(\mathbf{x},t) = \frac{\partial \varphi(\mathbf{x},t)}{\partial z} + \frac{\partial \psi_y(\mathbf{x},t)}{\partial x} - \frac{\partial \psi_x(\mathbf{x},t)}{\partial y}, \tag{8}$$

where the scalar and vector potentials φ and $\boldsymbol{\psi}$ satisfy the wave equations

$$\boldsymbol{\nabla}^2\varphi - \frac{1}{c_{\mathrm{L}}^2}\frac{\partial^2\varphi}{\partial t^2} = 0, \quad \boldsymbol{\nabla}^2\boldsymbol{\psi} - \frac{1}{c_{\mathrm{T}}^2}\frac{\partial^2\boldsymbol{\psi}}{\partial t^2} = 0, \quad \boldsymbol{\nabla}\cdot\boldsymbol{\psi} = 0, \quad \boldsymbol{\nabla}^2 \equiv \boldsymbol{\nabla}\cdot\boldsymbol{\nabla}. \tag{9}$$

Here, $c_{\mathrm{L}} = \sqrt{(\lambda + 2\mu)/\rho_{\mathrm{s}}}$ and $c_{\mathrm{T}} = \sqrt{\mu/\rho_{\mathrm{s}}}$ are the velocities of longitudinal and transversal waves, λ and μ are the Lamé elastic parameters, ρ_{s} is the material density of solid.

To solve the problem, we apply the complex integral Fourier transforms over space variables and time:

$$f^{\mathrm{F}}(\boldsymbol{k}, z, \omega) = \int_{-\infty}^{\infty}\int f(\mathbf{x}, t) e^{i(\omega t - \boldsymbol{k}\cdot\boldsymbol{\xi})}\, d\boldsymbol{\xi}\, dt\,, \tag{10}$$

$$f(\mathbf{x}, t) = \frac{1}{8\pi^3}\int_{-\infty}^{\infty}\int f^{\mathrm{F}}(\boldsymbol{k}, z, \omega) e^{-i(\omega t - \boldsymbol{k}\cdot\boldsymbol{\xi})}\, d\boldsymbol{k}\, d\omega\,, \tag{11}$$

where $\boldsymbol{k} = (k_x, k_y)$, $\boldsymbol{\xi} = (x, y)$, $d\boldsymbol{k} = dk_x\, dk_y$, $d\boldsymbol{\xi} = dx\, dy$. Then solving the problem in the Fourier transforms and returning to the originals, as it was shown earlier [9], we obtain

$$p_{\mathrm{rad}}(\mathbf{x}, t) = \mathbf{F}_0 \cdot \boldsymbol{\nabla} P_{\mathrm{rad}}(\mathbf{x}, t)\,, \tag{12}$$

$$p_{\mathrm{ref}}(\mathbf{x}, t) = \mathbf{F}_0 \cdot \boldsymbol{\nabla}^* P_{\mathrm{ref}}(\mathbf{x}, t)\,, \tag{13}$$

where $\boldsymbol{\nabla}^* = \boldsymbol{\nabla}_\perp - \mathbf{i}_z \partial/\partial z$ and

$$P_{\mathrm{rad}}(\mathbf{x}, t) = $$

$$= -\frac{1}{4\pi}\int_{-\infty}^{\infty}\int_{-\infty}^{\infty} G\left\{\boldsymbol{\xi} - \boldsymbol{\xi}', t - \frac{1}{c\alpha}\left[R_{\mathrm{w}}(\boldsymbol{\xi}', z - z_0) - \mathbf{M}_{\mathrm{w}}\cdot\boldsymbol{\xi}'\right]\right\} \times$$

$$\times \frac{d\boldsymbol{\xi}'}{R_{\mathrm{w}}(\boldsymbol{\xi}', z - z_0)}\,, \tag{14}$$

$$P_{\mathrm{ref}}(\mathbf{x}, t) = $$

$$= -\frac{1}{4\pi}\int_{-\infty}^{\infty}\int_{-\infty}^{\infty} G\left\{\boldsymbol{\xi} - \boldsymbol{\xi}', t - \frac{1}{c\alpha}\left[R_{\mathrm{w}}(\boldsymbol{\xi}', z + z_0) - \mathbf{M}_{\mathrm{w}}\cdot\boldsymbol{\xi}'\right]\right\} \times$$

$$\times \frac{R_{\mathrm{s}}(\boldsymbol{\xi}', z + z_0)\, d\boldsymbol{\xi}'}{R_{\mathrm{w}}(\boldsymbol{\xi}', z + z_0)}\,. \tag{15}$$

Here, $\boldsymbol{\xi}' = (x', y')$, $d\boldsymbol{\xi}' = dx'dy'$,

$$R_{\mathrm{w}}(\mathbf{x}) = \sqrt{\alpha_y x^2 + \alpha_x y^2 + \beta_{xy} xy + \alpha_{xy} z^2}, \quad R_{\mathrm{s}}(\mathbf{x}) = V^-(\mathbf{x})/V^+(\mathbf{x})\,,$$

$$V^{\pm}(\mathbf{x}) = \left[S_{\mathrm{T}}^2 - 2S^2(\mathbf{x})\right]^2 + 4S^2(\mathbf{x}) S_{z\mathrm{L}}(\mathbf{x}) S_{z\mathrm{T}}(\mathbf{x}) \pm$$

$$\pm N_{\mathrm{s}} S_{\mathrm{T}}^2 (c/c_{\mathrm{T}})^2 \left[1 - \mathbf{M}_{\mathrm{w}}\cdot\boldsymbol{\xi}/R_{\mathrm{w}}(\mathbf{x})\right]^2 S_{z\mathrm{L}}(\mathbf{x})/S_z(\mathbf{x})\,,$$

$$S(\mathbf{x}) = |\mathbf{S}(\mathbf{x})|, \qquad \mathbf{S}(\mathbf{x}) = \mathbf{r}(\boldsymbol{\xi})/R_{\mathrm{w}}(\mathbf{x}) - \mathbf{M}_{\mathrm{w}}\,,$$

$$\mathbf{r}(\boldsymbol{\xi}) = (\alpha_y x + \beta_{xy} y,\, \beta_{xy} x + \alpha_x y)\,,$$

$$S_{z\mathrm{A}}(\mathbf{x}) = \sqrt{S_{\mathrm{A}}^2 - S^2(\mathbf{x})}, \qquad S_{\mathrm{A}} = \alpha_{xy} c/c_{\mathrm{A}}, \qquad \mathrm{A} = \mathrm{L,T}\,,$$

$$S_z(\mathbf{x}) = \alpha_{xy} z/R_{\mathrm{w}}(\mathbf{x}), \qquad N_{\mathrm{s}} = \rho/\rho_{\mathrm{s}}, \qquad \mathbf{M}_{\mathrm{w}} = \mathbf{v}_{\mathrm{w}}/c\,,$$

$$\alpha_x = 1 - M_{\mathrm{w}x}^2, \quad \alpha_y = 1 - M_{\mathrm{w}y}^2, \quad \alpha_{xy} = 1 - M_{\mathrm{w}}^2, \quad \beta_{xy} = 2M_{\mathrm{w}x} M_{\mathrm{w}y}\,, \tag{16}$$

$R_s(\mathbf{x})$ is the reflection coefficient (as a function of angle spherical coordinates and physical-mechanical parameters of the acoustic and elastic media), $\mathbf{M}_w$ is the Mach number vector for wind.

Note that presentation (14) is exact, but presentation (15) is found as the inverse of Fourier transformations by making use of the stationary-phase approximation method [5]. Equation (15) does not imply the small contribution of the Rayleigh surface wave into the reflected field.

First, we consider a one-point source moving along the following road sections [11]: ***1***) $x < 0$, $y = -\xi_0$; ***2***) $\xi = \xi_0$, $3\pi/2 \le \theta \le \pi/2$; ***3***) $x = \xi_0$, $y > 0$. Then function $G(\boldsymbol{\xi}, t)$ may be represented as

$$G(\boldsymbol{\xi}, t) \equiv G^+(\boldsymbol{\xi}, t) = \left[G_1^+(\boldsymbol{\xi}, t) + G_2^+(\boldsymbol{\xi}, t) + G_3^+(\boldsymbol{\xi}, t)\right] e^{-i\Omega_0 t}, \tag{17}$$

where

$$G_1^+(\boldsymbol{\xi}, t) = \delta(x + x_0 - v_0 t)\delta(y + \xi_0)H(-x),$$

$$G_2^+(\boldsymbol{\xi}, t) = \delta(\xi - \xi_0)\delta\left[\xi_0(\theta - 3\pi/2) - v_0(t - t_0^+)\right]\left[H(\theta - 3\pi/2) - H(\theta - 2\pi)\right],$$

$$G_3^+(\boldsymbol{\xi}, t) = \delta(x - \xi_0)\delta\left[y - v_0(t - t_1^+)\right]H(y),$$

$$t_0^+ = x_0/v_0, \qquad t_1^+ = t_0^+ + (\pi/2)\xi_0/v_0 = s^+/v_0, \qquad s^+ = x_0 + (\pi/2)\xi_0. \tag{18}$$

In the case of opposite motion of the single-point acoustic source, i.e. along the road sections: ***1***) $y > 0$, $x = \xi_0$; ***2***) $\xi = \xi_0$, $3\pi/2 \le \theta \le 2\pi$; ***3***) $y = -\xi_0$, $x < 0$, we obtain:

$$G(\boldsymbol{\xi}, t) \equiv G^-(\boldsymbol{\xi}, t) = \left[G_1^-(\boldsymbol{\xi}, t) + G_2^-(\boldsymbol{\xi}, t) + G_3^-(\boldsymbol{\xi}, t)\right] e^{-i\Omega_0 t}, \tag{19}$$

where

$$G_1^-(\boldsymbol{\xi}, t) = \delta(x - \xi_0)\delta(y - y_0 + v_0 t)H(y),$$

$$G_2^-(\boldsymbol{\xi}, t) = \delta(\xi - \xi_0)\delta\left[\xi_0(2\pi - \theta) - v_0(t - t_0^-)\right]\left[H(\theta - 3\pi/2) - H(\theta - 2\pi)\right],$$

$$G_3^-(\boldsymbol{\xi}, t) = \delta\left[x + v_0(t - t_1^-)\right]\delta(y + \xi_0)H(-x),$$

$$t_0^- = y_0/v_0, \qquad t_1^- = t_0^- + (\pi/2)\xi_0/v_0 = s^-/v_0, \qquad s^- = y_0 + (\pi/2)\xi_0. \tag{20}$$

Here and above, $H(x)$ is the Heaviside step function, $v_0 > 0$ is the velocity of source motion on height $z = z_0$, Ω_0 is the circular frequency of sound radiation, $x_0 > 0$ is x-coordinate and $y_0 > 0$ is y-coodrinate of the sources at the time $t = 0$.

Substituting function $G(\boldsymbol{\xi}, t)$ into integrals (14) and (15), and applying the property of Dirac function [1]

$$\delta[f(x)] = \sum_j \frac{\delta(x - x_j)}{\left|f'(x_j)\right|}, \tag{21}$$

where x_j are the zeros of $f(x)$, $f'(x_j)$ is the derivative of $f(x)$ over x in point $x = x_j$, as well as the formula

$$\int_a^b f(x')\delta(x - x')\,dx' = f(x)[H(x - a) - H(x - b)], \tag{22}$$

we calculate the acoustic potentials in radiated and reflected waves $P_{\rm rad}(\mathbf{x},t)$ and $P_{\rm ref}(\mathbf{x},t)$ for these cases as follows:

$$P_q^+(\mathbf{x},t) \equiv P_q^+(\mathbf{x},x_0,\xi_0,t,v_0,\Omega_0)\,e^{-i\Omega_0 t},$$

$$P_q^-(\mathbf{x},t) \equiv P_q^-(\mathbf{x},y_0,\xi_0,t,v_0,\Omega_0)\,e^{-i\Omega_0 t}, \quad q = \text{rad},\text{ref}, \tag{23}$$

where

$$\begin{aligned} P_q^+(\boldsymbol{\xi},z_q,t,\xi_0,x_0,v_0,\Omega_0) &= P_{q,1}^+(x+x_0-v_0t,y+\xi_0,z_q,\Omega_0)\times \\ &\times H\big[x_0-v_0t+\varepsilon_1^+L_1^+(x+x_0-v_0t,y+\xi_0,z_q)\big]+ \\ &+P_{q,2}^+(\boldsymbol{\xi},z_q,t,\Omega_0)\{H[\theta^+(\boldsymbol{\xi},z_q,t)-3\pi/2]- \\ &-H[\theta^+(\boldsymbol{\xi},z_q,t)-2\pi]\}+P_{q,3}^+(x-\xi_0,y+s^+-v_0t,z_q,\Omega_0)\times \\ &\times H\big[-(s^+-v_0t)-\varepsilon_3^+L_3^+(x-\xi_0,y+s^+-v_0t,z_q)\big], \end{aligned} \tag{24}$$

$$\begin{aligned} P_q^-(\boldsymbol{\xi},z_q,t,\xi_0,x_0,v_0,\Omega_0) &= P_{q,1}^-(x-\xi_0,y-y_0+v_0t,z_q,\Omega_0)\times \\ &\times H\big[y_0-v_0t+\varepsilon_1^-L_1^-(x-\xi_0,y-y_0+v_0t,z_q)\big]+ \\ &+P_{q,2}^-(\boldsymbol{\xi},z_q,t,\Omega_0)\{H[\theta^-(\boldsymbol{\xi},z_q,t)-3\pi/2]- \\ &-H[\theta^-(\boldsymbol{\xi},z_q,t)-2\pi]\}+P_{q,3}^-(x-s^-+v_0t,y+\xi_0,z_q,\Omega_0)\times \\ &\times H\big[-(s^--v_0t)-\varepsilon_3^-L_3^-(x-s^-+v_0t,y+\xi_0,z_q)\big]. \end{aligned} \tag{25}$$

In these formulas

$$z_{\rm rad} = z-z_0, \qquad z_{\rm ref} = z+z_0,$$

$$P_{{\rm rad},m}^{\pm}(\mathbf{x},\Omega_0) = -\exp\big[{\rm i}K_m^{\pm}L_m^{\pm}(\mathbf{x})\big]/\big(4\pi R_m^{\pm}(\mathbf{x})\big),$$

$$P_{{\rm ref},m}^{\pm}(\mathbf{x},\Omega_0) = -R_{\rm s}(\mathbf{x})\exp\big[{\rm i}K_m^{\pm}L_m^{\pm}(\mathbf{x})\big]/(4\pi R_m^{\pm}(\mathbf{x})), \qquad m=1,3,$$

$$P_{{\rm rad},2}^{\pm}(\mathbf{x},t,\Omega_0) = -\exp\big[{\rm i}K_2L_2^{\pm}(\mathbf{x},t)\big]/\big(4\pi R_m^{\pm}(\mathbf{x})\big),$$

$$P_{{\rm ref},2}^{\pm}(\mathbf{x},t,\Omega_0) = -R_{\rm s}(\mathbf{x},t)\exp\big[{\rm i}K_2L_2^{\pm}(\mathbf{x},t)\big]/(4\pi R_2^{\pm}(\mathbf{x},t)), \tag{26}$$

and

$$R_m^{\pm}(\mathbf{x}) = \sqrt{\alpha_{y,m}^{\pm}x^2+\alpha_{x,m}^{\pm}y^2+2\beta_{xy,m}^{\pm}xy+\alpha_{xy,m}^{\pm}z^2},$$

$$L_m^{\pm}(\mathbf{x}) = R_m^{\pm}(\mathbf{x})-M_{{\rm w}x,m}^{\pm}x-M_{{\rm w}y,m}^{\pm}y, \qquad m=1,3,$$

$$\begin{aligned} R_2^{\pm}(\mathbf{x},t) &= \{R_{\rm w}(\boldsymbol{\xi}-\boldsymbol{\xi}',z)\big[1-\varepsilon_2M_{\rm w}\sin(\theta'-\theta_{\rm w})\big]+ \\ &+\varepsilon_2\big[r_x(\boldsymbol{\xi}-\boldsymbol{\xi}')\sin\theta'-r_y(\boldsymbol{\xi}-\boldsymbol{\xi}')\cos\theta'\big]\}\big|_{\xi'=\xi_0,\theta'=\theta_0^{\pm}(t)}, \end{aligned}$$

$$L_2^{\pm}(\mathbf{x},t) = \big[R_w(\boldsymbol{\xi}-\boldsymbol{\xi}',z)-\mathbf{M}_w\cdot(\boldsymbol{\xi}-\boldsymbol{\xi}')\big]\big|_{\xi'=\xi_0,\theta'=\theta_0^{\pm}(t)}, \tag{27}$$

with the parameters

$$\alpha_{x,m}^{\pm} = 1-(M_{wx,m}^{\pm})^2, \qquad \alpha_{y,m}^{\pm} = 1-(M_{wy,m}^{\pm})^2,$$

$$\alpha^{\pm}_{xy,m} = 1 - (M^{\pm}_{\mathrm{w}x,m})^2 - (M^{\pm}_{\mathrm{w}y,m})^2, \qquad \beta^{\pm}_{xy,m} = M^{\pm}_{\mathrm{w}x,m} M^{\pm}_{\mathrm{w}y,m},$$

$$K^{\pm}_m = K_0/\alpha^{\pm}_{xy,m}, \qquad \varepsilon^{\pm}_m = M_0/\alpha^{\pm}_{xy,m}, \qquad m = 1,3,$$

$$K_2 = K_0/\alpha_{xy}, \qquad \varepsilon_2 = M_0/\alpha_{xy},$$

$$M^{+}_{\mathrm{w}x,1} = M_{\mathrm{w}x} - M_0, \qquad M^{+}_{\mathrm{w}y,1} = M_{\mathrm{w}y}, \qquad M^{+}_{\mathrm{w}x,3} = M_{\mathrm{w}x},$$

$$M^{+}_{\mathrm{w}y,3} = M_{\mathrm{w}y} - M_0, \qquad M^{-}_{\mathrm{w}x,1} = M_{\mathrm{w}x}, \qquad M^{-}_{\mathrm{w}y,1} = M_{\mathrm{w}y} + M_0,$$

$$M^{-}_{\mathrm{w}x,3} = M_{\mathrm{w}x} + M_0, \qquad M^{-}_{\mathrm{w}y,3} = M_{\mathrm{w}y},$$

$$\theta^{\pm}(\mathbf{x},t) = \theta^{\pm}_0(t) - (\varepsilon/\xi_0) L^{\pm}_2(\mathbf{x},t),$$

$$\theta^{+}_0(t) = 3\pi/2 + (v_0 t - x_0)/\xi_0, \qquad \theta^{-}_0(t) = 2\pi - (v_0 t - y_0)/\xi_0. \tag{28}$$

Note that zeros x_j for the case of straight road sections are obtained exactly, but for the case of curved road section, they are found using the iterative technique of solution of corresponding transcendental equations by the method described in our previous work [9]. Substituting functions $P^{\pm}_{\mathrm{rad}}(\mathbf{x},t)$ and $P^{\pm}_{\mathrm{ref}}(\mathbf{x},t)$ into (12) and (13), we obtain the expressions for acoustic pressure in waves radiated from single sources moving in two opposite directions, and reflected from the surface of elastic half-space:

$$p^{+}_{\mathrm{tot}}(\mathbf{x},t,\xi_0,x_0,z_0,v_0,\Omega_0,\mathbf{F}_0) = \left[p^{+}_{\mathrm{rad}}(\boldsymbol{\xi},z-z_0,t,\xi_0,x_0,v_0,\Omega_0,\mathbf{F}_0) + \right.$$

$$\left. + p^{+}_{\mathrm{ref}}(\boldsymbol{\xi},z+z_0,t,\xi_0,x_0,v_0,\Omega_0,\mathbf{F}_0)\right] e^{-i\Omega_0 t}, \tag{29}$$

$$p^{-}_{\mathrm{tot}}(\mathbf{x},t,\xi_0,y_0,z_0,v_0,\Omega_0,\mathbf{F}_0) = \left[p^{-}_{\mathrm{rad}}(\boldsymbol{\xi},z-z_0,t,\xi_0,y_0,v_0,\Omega_0,\mathbf{F}_0) + \right.$$

$$\left. + p^{-}_{\mathrm{ref}}(\boldsymbol{\xi},z+z_0,t,\xi_0,y_0,v_0,\Omega_0,\mathbf{F}_0)\right] e^{-i\Omega_0 t}, \tag{30}$$

where

$$p^{+}_q(\boldsymbol{\xi},z_q,t,\xi_0,x_0,v_0,\Omega_0,\mathbf{F}_0) = iK_0\mathbf{F}_0 \cdot \left\langle \mathbf{A}^{+}_{q,1}(x+x_0-v_0t, y+\xi_0, z_{\mathrm{q}},\Omega_0) \times \right.$$

$$\times P^{+}_{q,1}(x+x_0-v_0t, y+\xi_0, z_q,\Omega_0) \times$$

$$\times H\left[x_0 - v_0t + \varepsilon^{+}_1 L^{+}_1(x+x_0-v_0t, y+\xi_0, z_q)\right] +$$

$$+ \mathbf{A}^{+}_{q,2}(\boldsymbol{\xi},z_q,t,\Omega_0) P^{+}_{q,2}(\boldsymbol{\xi},z_q,t,\Omega_0) \times$$

$$\times \left\{H\left[\theta^{+}(\boldsymbol{\xi},z_q,t) - 3\pi/2\right] - H\left[\theta^{+}(\boldsymbol{\xi},z_q,t) - 2\pi\right]\right\} +$$

$$+ \mathbf{A}^{+}_{q,3}(x-\xi_0, y+s^{+}-v_0t, z_{\mathrm{q}},\Omega_0) \times$$

$$\times P^{+}_{q,3}(x-\xi_0, y+s^{+}-v_0t, z_q,\Omega_0) \times$$

$$\left. \times H\left[-(s^{+}-v_0t) - \varepsilon^{+}_3 L^{+}_3(x-\xi_0, y+s^{+}-v_0t, z_q)\right]\right\rangle, \tag{31}$$

$$p^{-}_q(\boldsymbol{\xi},z_q,t,\xi_0,y_0,v_0,\Omega_0,\mathbf{F}_0) = iK_0\mathbf{F}_0 \cdot \left\langle \mathbf{A}^{-}_{q,1}(x-\xi_0, y-y_0+v_0t, z_q,\Omega_0) \times \right.$$

$$\times P^{+}_{q,1}(x-\xi_0, y-y_0+v_0t, z_q,\Omega_0) \times$$

$$\times H\left[y_0 - v_0 t + \varepsilon_1^- L_1^-(x-\xi_0, y - y_0 + v_0 t, z_q)\right] +$$

$$+ \mathbf{A}_{q,2}^-(\boldsymbol{\xi}, z_q, t, \Omega_0) P_{q,2}^-(\boldsymbol{\xi}, z_q, t, \Omega_0) \times$$

$$\times \left\{H\left[\theta^-(\boldsymbol{\xi}, z_q, t) - 3\pi/2\right] - H\left[\theta^-(\boldsymbol{\xi}, z_q, t) - 2\pi\right]\right\} +$$

$$+ \mathbf{A}_{q,3}^-(x - s^- + v_0 t, y + \xi_0, z_{\mathrm{q}}, \Omega_0) \times$$

$$\times P_{q,3}^-(x - s^- + v_0 t, y + \xi_0, z_q, \Omega_0) \times$$

$$\times H\left[-(s^- - v_0 t) - \varepsilon_3^- L_3^-(x - s^- + v_0 t, y + \xi_0, z_{\mathrm{q}})\right]\Big\rangle \qquad (32)$$

with

$$\mathbf{A}_{\mathrm{rad},\ell}^{\pm}(\mathbf{x}, t, \Omega_0) = \left\{A_{x,\ell}^{\pm}(\mathbf{x}, \Omega_0), A_{y,\ell}^{\pm}(\mathbf{x}, \Omega_0), A_{z,\ell}^{\pm}(\mathbf{x}, \Omega_0, t)\right\},$$

$$\mathbf{A}_{\mathrm{ref},\ell}^{\pm}(\mathbf{x}, t, \Omega_0) = \left\{A_{x,\ell}^{\pm}(\mathbf{x}, \Omega_0), A_{y,\ell}^{\pm}(\mathbf{x}, \Omega_0), -A_{z,\ell}^{\pm}(\mathbf{x}, \Omega_0, t)\right\}, \ \ell = 1,2,3, \qquad (33)$$

and

$$A_{\alpha,m}^{\pm}(\mathbf{x}, \Omega_0) = -\frac{1}{\alpha_{xy,m}^{\pm}}\left\{M_{\mathrm{w}\alpha,m}^{\pm} - \frac{r_{\alpha,m}^{\pm}(\boldsymbol{\xi})}{R_m^{\pm}(\mathbf{x})}\left[1 - \frac{1}{iK_m^{\pm}R_m^{\pm}(\mathbf{x})}\right]\right\},$$

$$A_{z,m}^{\pm}(\mathbf{x}, \Omega_0) = \frac{z}{R_m^{\pm}(\mathbf{x})}\left[1 - \frac{1}{iK_m^{\pm}R_m^{\pm}(\mathbf{x})}\right],$$

$$A_{\alpha,2}^{\pm}(\mathbf{x}, \Omega_0, t) = -\frac{1}{\alpha_{xy}}\Bigg\langle M_{\mathrm{w}\alpha} - \Bigg\{\frac{r_\alpha^{\pm}(\boldsymbol{\xi}, t)}{R_2^{\pm}(\mathbf{x}, t)}\left\{1 \mp M_{\mathrm{w}}\varepsilon_2 \sin\left[\theta_0^{\pm}(t) - \theta_{\mathrm{w}}\right]\right\} \pm$$

$$\pm \varepsilon_2 r_\alpha\left[\sin\theta_0^{\pm}(t) - \cos\theta_0^{\pm}(t)\right]\left[1 - \frac{1}{iK_2R_2^{\pm}(\mathbf{x}, t)}\right]\Bigg\}\Bigg\rangle,$$

$$r_\alpha^{\pm}(\boldsymbol{\xi}, t) = r_\alpha(\boldsymbol{\xi} - \boldsymbol{\xi}')\big|_{\xi'=\xi_0, \theta'=\theta_0^{\pm}(t)}, \qquad \alpha = x, y, \qquad m = 1,3. \qquad (34)$$

In the particular case of monopole sound source, the vector $\mathbf{F}_0$ has only one radial component $\mathbf{F}_0 = F_0\mathbf{i}_R$ in the moving spherical coordinates associated with a location of this source in an acoustical medium and its mirror image in an elastic half-space, where $\mathbf{i}_R$ is the unit vector.

Then in the moving Cartesian coordinates of this source and its mirror image, we obtain, e. g.

$$\mathbf{i}_R = \frac{(x + x_0 - v_0 t)\mathbf{i}_x + (y + \xi_0)\mathbf{i}_y + (z - z_0)\mathbf{i}_y}{R(x + x_0 - v_0 t, y + \xi_0, z - z_0)},$$

$$\mathbf{i}_R = \frac{(x + x_0 - v_0 t)\mathbf{i}_x + (y + \xi_0)\mathbf{i}_y - (z + z_0)\mathbf{i}_y}{R(x + x_0 - v_0 t, y + \xi_0, z + z_0)}, \qquad (35)$$

where $R(\mathbf{x}) = \sqrt{x^2 + y^2 + z^2}$.

After some simplifications, the formulae (31) and (32) can be given as

$$p_q^+(\boldsymbol{\xi}, z_q, t, \xi_0, x_0, v_0, \Omega_0, \mathbf{F}_0) = -K_0F_0\Big\langle B_1^+(x + x_0 - v_0 t, y + \xi_0, z_q, \Omega_0) \times$$

$$\times P_{q,1}^+(x + x_0 - v_0 t, y + \xi_0, z_q, \Omega_0) \times$$

$$\times H\left[x_0 - v_0 t + \varepsilon_1^+ L_1^+ (x + x_0 - v_0 t, y + \xi_0, z_q)\right] +$$

$$+ B_2^+ (\boldsymbol{\xi}, z_q, t, \Omega_0) P_{q,2}^+ (\boldsymbol{\xi}, z_q, t, \Omega_0) \times$$

$$\times \left\{H\left[\theta^+ (\boldsymbol{\xi}, z_q, t) - 3\pi / 2\right] - H\left[\theta^+ (\boldsymbol{\xi}, z_q, t) - 2\pi\right]\right\} +$$

$$+ B_3^+ (x - \xi_0, y + s^+ - v_0 t, z_q, \Omega_0) \times$$

$$\times P_{q,3}^+ (x - \xi_0, y + s^+ - v_0 t, z_q, \Omega_0) \times$$

$$\times H\left[-(s^+ - v_0 t) - \varepsilon_3^+ L_3^+ (x - \xi_0, y + s^+ - v_0 t, z_q)\right]\Big\rangle, \qquad (36)$$

$$p_q^- (\boldsymbol{\xi}, z_q, t, \xi_0, y_0, v_0, \Omega_0, \mathbf{F}_0) = -K_0 F_0 \Big\langle B_1^- (x - \xi_0, y - y_0 + v_0 t, z_q, \Omega_0) \times$$

$$\times P_{q,1}^+ (x - \xi_0, y - y_0 + v_0 t, z_q, \Omega_0) \times$$

$$\times H\left[y_0 - v_0 t + \varepsilon_1^- L_1^- (x - \xi_0, y - y_0 + v_0 t, z_q)\right] +$$

$$+ B_2^- (\boldsymbol{\xi}, z_q, t, \Omega_0) P_{q,2}^- (\boldsymbol{\xi}, z_q, t, \Omega_0) \times$$

$$\times \left\{H\left[\theta^- (\boldsymbol{\xi}, z_q, t) - 3\pi / 2\right] - H\left[\theta^- (\boldsymbol{\xi}, z_q, t) - 2\pi\right]\right\} +$$

$$+ B_3^- (x - s^- + v_0 t, y + \xi_0, z_q, \Omega_0) \times$$

$$\times P_{q,3}^- (x - s^- + v_0 t, y + \xi_0, z_q, \Omega_0) \times$$

$$\times H\left[-(s^- - v_0 t) - \varepsilon_3^- L_3^- (x - s^- + v_0 t, y + \xi_0, z_q)\right]\Big\rangle, \qquad (37)$$

where

$$B_m^\pm (\mathbf{x}, \Omega_0) = -\frac{1 - iK_m^\pm L_m^\pm (\mathbf{x})}{K_0 R(\mathbf{x})}, \quad m = 1, 3,$$

$$B_2^\pm (\mathbf{x}, t, \Omega_0) = -\frac{1 - iK_2 L_2^\pm (\mathbf{x}, t)}{K_0 R^\pm (\mathbf{x}, t)}, \quad R^\pm (\mathbf{x}, t) = R(\boldsymbol{\xi} - \boldsymbol{\xi}', z)\big|_{\xi' = \xi_0, \theta' = \theta_0^\pm (t)}. \qquad (38)$$

2. Numerical analysis of acoustic field and discussion. In the case when many sound sources move in each direction, we should replace initial positions x_0 and y_0 in the foregoing formulas by x_j and y_j, where $j = -n, -(n-1), \ldots, -1, 0, 1, \ldots, m-1, m$, $n > 0$, $m > 0$, i. e. at present, we have $2(n + m + 1)$ sources.

Let the distances between the sources on straight road sections be equal to Δ. Then instead of $x_0 = x_j$ and $y_0 = y_j$, they can be written as $x_0 = j\Delta$ and $y_0 = j\Delta$, respectively.

Suppose that in each direction of motion, the three lanes are as follows: two lanes along which personal cars travel at intervals between them being $\Delta_{\mathrm{L}\ell}$, $\ell = 1, 2$, and at the same velocity v_{L} (ξ_0 is replaced by $\xi_{\mathrm{L}\ell}^\pm = \xi_0 \pm \xi_{\mathrm{L}\ell}$, $\ell = 1, 2$), and the third lane on which heavy trucks travel at distances between them being Δ_{C} and velocity v_{C} (ξ_0 is replaced by $\xi_{\mathrm{C}}^\pm = \xi_0 \pm \xi_{\mathrm{C}}$). Similarly, we replace numbers m and n by $m_{\mathrm{L}\ell}$ and $n_{\mathrm{L}\ell}$, $\ell = 1, 2$, for personal cars, and by m_{C} and n_{C} for heavy trucks.

Applying the mentioned changes in the formulas for acoustic pressure and summarizing the contributions of all particular sound sources, we can analyze the acoustic field near the bend in the dual carriageway road composed of six lanes taking the wind impact into consideration:

$$p_{\mathrm{tot}}(\mathbf{x},t) = \sum_{j=-n_{\mathrm{L}}}^{m_{\mathrm{L}}} \sum_{\ell=1}^{2} \left[p_{\mathrm{tot}}^{+}(\mathbf{x},t,\xi_{\mathrm{L}\ell}^{+}, j\Delta_{\mathrm{L}\ell}, h_{\mathrm{L}}, v_{\mathrm{L}}, \Omega_{\mathrm{L}}, \mathbf{F}_{\mathrm{L}}) + \right.$$

$$+ \left. p_{\mathrm{tot}}^{-}(\mathbf{x},t,\xi_{\mathrm{L}\ell}^{-}, j\Delta_{\mathrm{L}\ell}, h_{\mathrm{L}}, v_{\mathrm{L}}, \Omega_{\mathrm{L}}, \mathbf{F}_{\mathrm{L}}) \right] +$$

$$+ \sum_{j=-n_{\mathrm{C}}}^{m_{\mathrm{C}}} \left[p_{\mathrm{tot}}^{+}(\mathbf{x},t,\xi_{\mathrm{C}}^{+}, j\Delta_{\mathrm{C}}, h_{\mathrm{C}}, v_{\mathrm{C}}, \Omega_{\mathrm{C}}, \mathbf{F}_{\mathrm{C}}) + \right.$$

$$+ \left. p_{\mathrm{tot}}^{-}(\mathbf{x},t,\xi_{\mathrm{C}}^{-}, j\Delta_{\mathrm{C}}, h_{\mathrm{C}}, \Omega_{\mathrm{C}}, \mathbf{F}_{\mathrm{C}}) \right]. \tag{39}$$

The instantaneous acoustic pressure level from the considered sources of noise is obtained on the basis of the formula (in dB or phones)

$$I(\mathbf{x},t) = 20 \lg\left(\frac{|p_{\mathrm{tot}}(\mathbf{x},t)|}{p_0} \right), \tag{40}$$

where $p_0 = 2 \cdot 10^{-5}$ Pa is the threshold pressure.

The other energetic characteristic (as a result of noise analysis) is the acoustic pressure level averaged over time period T_0 (in dB)

$$I_{\mathrm{av}}(\mathbf{x}) = 10 \lg\left\{ \frac{1}{T_0} \int_{-T_0/2}^{T_0/2} \left[\frac{|p_{\mathrm{tot}}(\mathbf{x},t)|}{p_0} \right]^2 dt \right\}, \tag{41}$$

where, for example, $T_0 = 2\pi/\Omega_0$.

The analysis of acoustic pressure in radiated and reflected waves is carried out using (29), (30), (36)–(39), i.e. for a monopole sound sources with $\mathbf{F}_{\mathrm{A}} = F_{\mathrm{A}} \mathbf{i}_R$ $(\mathrm{A} = \mathrm{L}, \mathrm{C})$.

It can be shown that

$$F_{\mathrm{A}} K_{\mathrm{A}} = 4\pi \cdot 10^{I_{\mathrm{A}}/20} p_0 \cdot 1\,\mathrm{metre}, \tag{42}$$

where I_{A} is the average acoustic pressure level measured at the one-metre distance from individual A-type source, $K_{\mathrm{A}} = \Omega_{\mathrm{A}}/c$ $(\mathrm{A} = \mathrm{L}, \mathrm{C})$.

For numerical calculations, we take $I_{\mathrm{L}} = 75\,\mathrm{dB}$ for personal cars and $I_{\mathrm{C}} = 85\,\mathrm{dB}$ for heavy transport [4, 7]. The vehicles move in air medium with density $\rho = 1.293\,\mathrm{kg/m^3}$ and sound speed $c = 331\,\mathrm{m/s}$. The road is coated by asphalt with material density $\rho_{\mathrm{s}} = 2000\,\mathrm{kg/m^3}$ and velocities of longitudinal and transversal waves $c_{\mathrm{L}} = 3468\,\mathrm{m/s}$, $c_{\mathrm{T}} = 1667\,\mathrm{m/s}$ [6, 15]. The chosen frequencies of source vibrations are $\Omega_{\mathrm{L}} = 300\,\mathrm{Hz}$ for personal vehicles and $\Omega_{\mathrm{C}} = 250\,\mathrm{Hz}$ for heavy trucks [6]. The heights of sources are $h_{\mathrm{L}} = 1\,\mathrm{m}$ and $h_{\mathrm{C}} = 2\,\mathrm{m}$, respectively.

In the model situation, we consider a road with a bend as in the Textile Workers Avenue in Łódź (Poland), the radius of which is $\xi_0 = 152\,\mathrm{m}$, with distances from the road axis on both sides to the first, second and third lane being $\xi_{\mathrm{L}1} = 3\,\mathrm{m}$, $\xi_{\mathrm{L}2} = 6\,\mathrm{m}$ and $\xi_{\mathrm{C}} = 10\,\mathrm{m}$, respectively. From the observations carried out between 10 and 11 a.m. on 22 June 2011 it was calculated that

1255 personal cars and 151 heavy vehicles moved in both directions*. Taking approximately small distances along straight sections of the carriageway from bend in the road along which the vehicles travel at the same velocity, $v_0 = v_L = v_C = 40\,\text{km/h}$, we obtain the following values for the number of vehicles $m_{L1} = m_{L2} = n_{L1} = n_{L2} = 10$, $m_C = n_C = 2$, $\Delta_{L1} = \Delta_{L2} = 64\,\text{m}$, $\Delta_C = 264\,\text{m}$. The calculations are mainly done for height $z = 4\,\text{m}$.

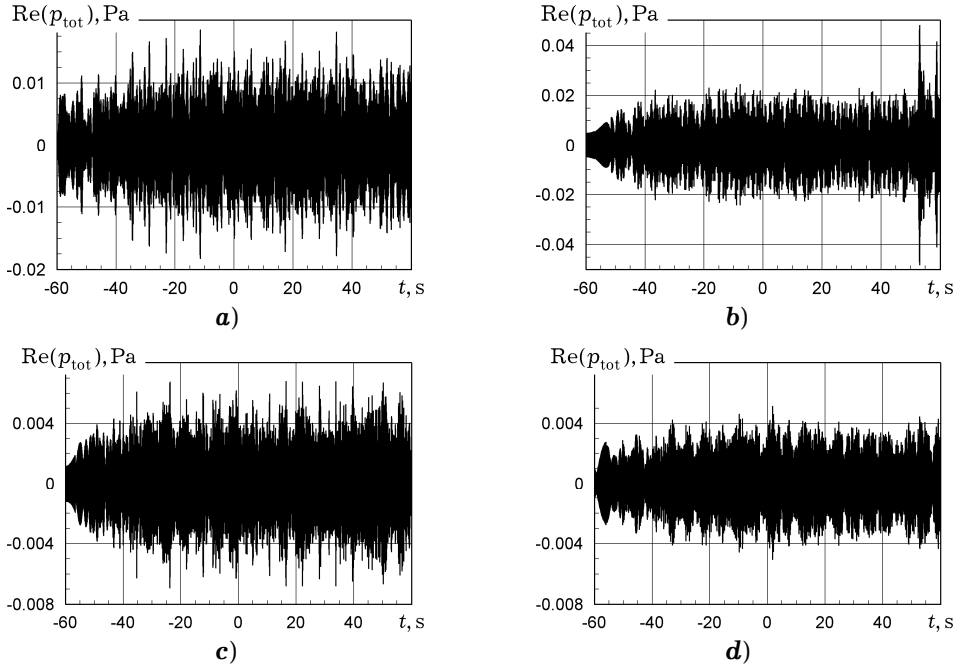

Fig. 1. Acoustic pressure $\text{Re}(p_{tot})$ on height $z = 4\,\text{m}$ vs. time in windless conditions on the bisector of road bend: ***a***) in the center of curved road section $x = y = 0$; ***b***) $x = -y = 152\,\text{m}$; ***c***) $x = -y = 304\,\text{m}$; ***d***) $x = -y = 456\,\text{m}$.

The structure of total acoustic pressure $\text{Re}(p_{tot})$ (in Pa) is displayed in Fig. 1 as a function of time for windless conditions on the different radii with the origin in the road arc center and for $\theta = 315^\circ$ (i.e. on the axis of geometric symmetry of this road section). The signals are calculated in the four points during 120 s. Because of non-symmetrical conditions of vehicle motion, the structure of acoustic pulses calculated in the two points, $\xi = 0$ and $\xi = 304\,\text{m}$, symmetrical about the road axis, is different. It is also shown that in these points, the amplitudes of signals are smaller than the ones on the road axis. In turn, on the road axis, the signals are more separated as compared to the signals on the road periphery. The strong acoustic signals are generated by heavy transport, while lesser pulses are radiated by personal cars.

Fig. 2 illustrates the impact of wind velocity ($v_w = 20\,\text{km/h}$ and $v_w = 40\,\text{km/h}$) on the structure of acoustic pressure calculated at the distance of 40 m from the axis of bend in the road ($x = -y = 192\,\text{m}$). It follows from this illustration that an increment of wind velocity causes a 'diffusion' of the signal in time. It is worth noting that in these conditions, the acoustic pressure radiated from personal cars is increased too.

* The observations were done by students of Lodz University of Technology Mariola Mądra and Paulina Midera.

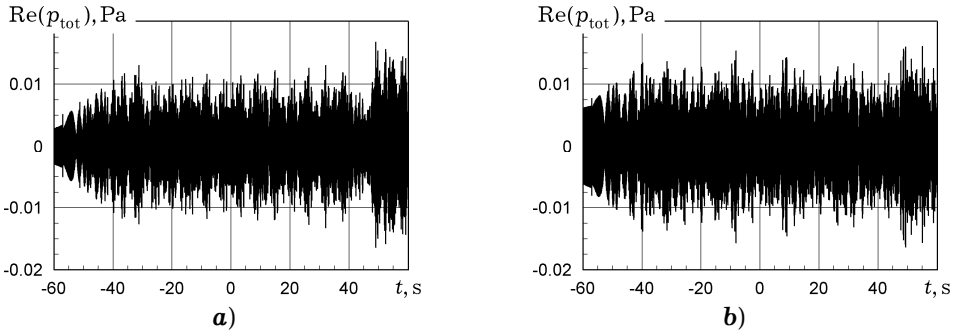

a) ***b***)

Fig. 2. Acoustic pressure $\mathrm{Re}(p_{\mathrm{tot}})$ at the distance of 40 m from the road bend ($x = -y = 192\,\mathrm{m}$) vs. time taking wind velocity into consideration: ***a***) $v_{\mathrm{w}} = 20\,\mathrm{km/h}$; ***b***) $v_{\mathrm{w}} = 40\,\mathrm{km/h}$ ($\theta_{\mathrm{w}} = 315^{\circ}$).

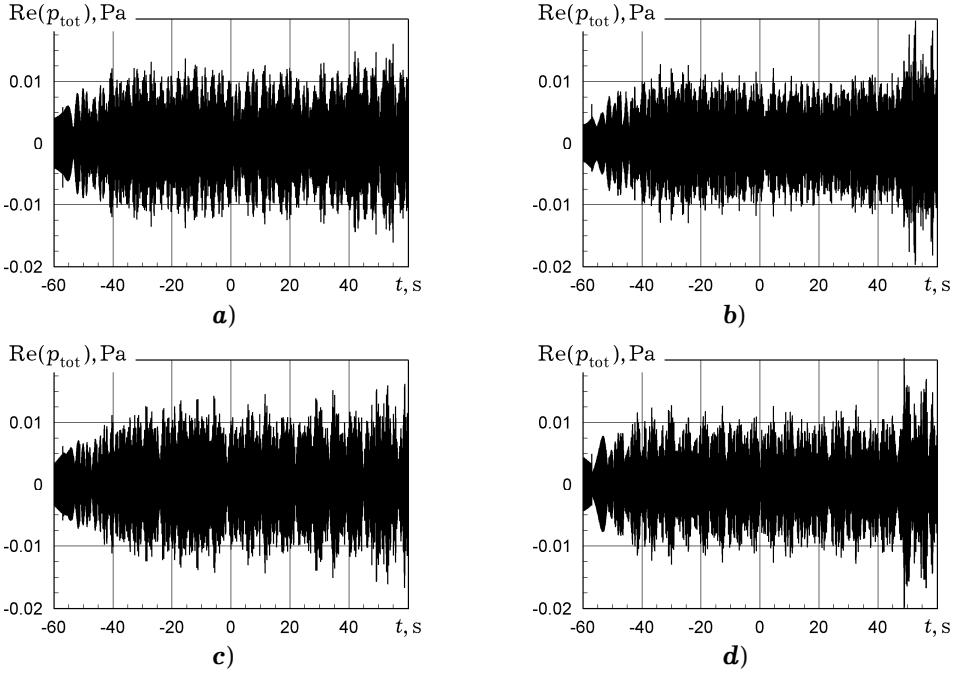

a) ***b***)

c) ***d***)

Fig. 3. Acoustic pressure $\mathrm{Re}(p_{\mathrm{tot}})$ at the distance of 40 m from the road bend ($x = -y = 192\,\mathrm{m}$) vs. time taking wind direction into consideration ($v_{\mathrm{w}} = 40$ km/h): ***a***) $\theta_{\mathrm{w}} = 0^{\circ}$; ***b***) $\theta_{\mathrm{w}} = 180^{\circ}$; ***c***) $\theta_{\mathrm{w}} = 45^{\circ}$; ***d***) $\theta_{\mathrm{w}} = 225^{\circ}$.

Similar effects are observed in the structure of signals radiated from vehicles on a roundabout [9]. Thus, the influence of wind parameters on radiated sound signals is evident.

The effect of wind direction on the structure of acoustic signals is shown in Figs. 3 and 4. The value of $\mathrm{Re}(p_{\mathrm{tot}})$ is calculated also at the distance of 40 m from the road axis ($x = -y = 192\,\mathrm{m}$) as a function of time with wind velocity $v_{\mathrm{w}} = 40\,\mathrm{km/h}$ for the four mutually opposite wind directions, namely, $\theta_{\mathrm{w}} = 0\,^{\circ}$ and 180°, 45° and 225°, 90° and 270°, 315° and 135° This also shows a sufficient influence of wind direction on the structure of sound waves. However, in both considered cases the amplitudes of acoustic pressure do not change considerably, i.e. the effect of wind parameters has a local character.

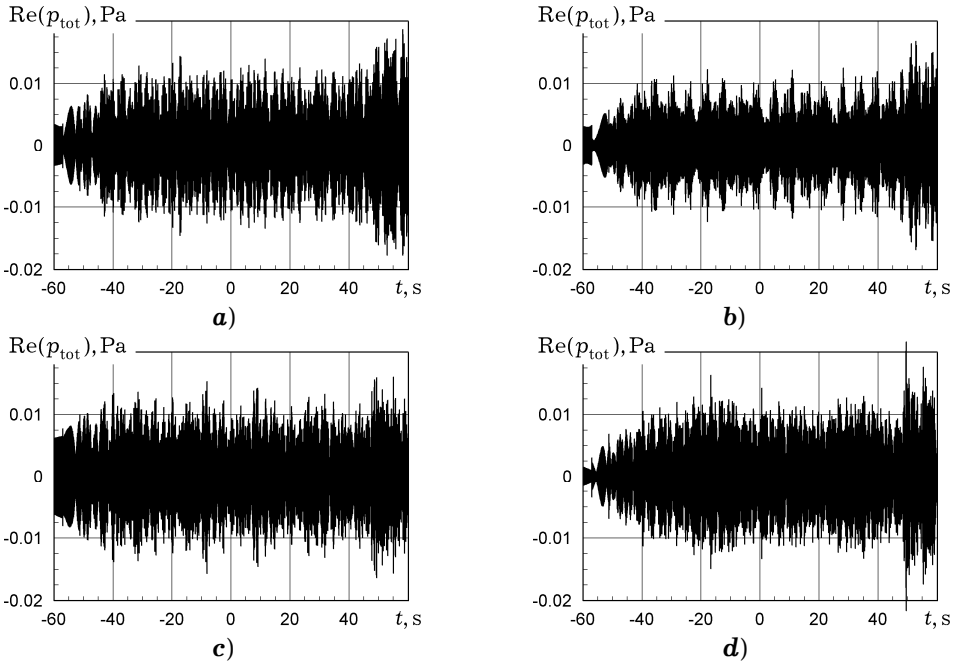

Fig. 4. Acoustic pressure $\mathrm{Re}(p_{\mathrm{tot}})$ at the distance of 40 m from the road bend ($x = -y = 192\,\mathrm{m}$) vs. time taking wind direction into consideration ($v_{\mathrm{w}} = 40$ km/h): ***a***) $\theta_{\mathrm{w}} = 90^{\circ}$; ***b***) $\theta_{\mathrm{w}} = 270^{\circ}$; ***c***) $\theta_{\mathrm{w}} = 315^{\circ}$; ***d***) $\theta_{\mathrm{w}} = 135^{\circ}$.

Figure 5 shows the distribution of acoustic pressure level in space $I(x, y) \equiv I(x, y, t)$ (in dB) for $t = 20\,\mathrm{s}$, calculated by (39) and (40). From the calculations carried out in windy conditions ($v_{\mathrm{w}} = 40\,\mathrm{km/h}$, $\theta_{\mathrm{w}} = 315\,^{\circ}$) it follows that noise propagation is characterized by a high acoustic pressure level (near 70 dB) over straight road and curved road section.

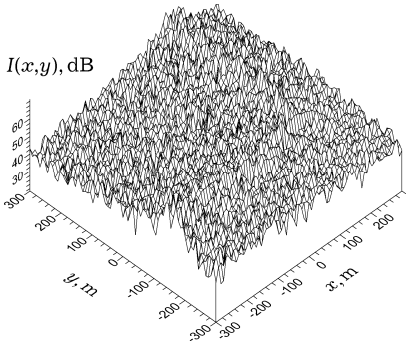

Fig. 5. Sound intensity distribution in space $I(x, y) = 20\log(|p_{\mathrm{tot}}|/p_0)$ in the moment of time $t = 0\,\mathrm{s}$ on the square $300 \times 300\,\mathrm{m}^2$, $z = 4\,\mathrm{m}$ for $v_{\mathrm{w}} = 40$ km/h and $\theta_{\mathrm{w}} = 315^{\circ}$.

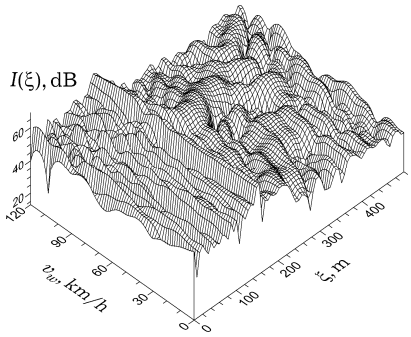

Fig. 6. Sound intensity distribution $I(\xi) = 20\log(|p_{\mathrm{tot}}|/p_0)$ along bisector $0 \le \xi \le 500\,\mathrm{m}$, $\theta = 315^{\circ}$ as a function of wind velocity v_{w} ($\theta_{\mathrm{w}} = 315^{\circ}$) in the moment of time $t = 0\,\mathrm{s}$.

In Figs. 6–8, the distributions of sound intensity $I(x, y)$ are displayed along bisector $0 \le \xi \le 500\,\mathrm{m}$, $\theta = 315\,^{\circ}$ for different velocities v_{w} ($\theta_{\mathrm{w}} = 315\,^{\circ}$)

and directions θ_w ($v_w = 40$ km/h) of wind, and also for different velocities of vehicles v_0 ($v_w = 40$ km/h, $\theta_w = 315°$). It is shown that the effects of wind and car motion on sound intensity structure is the biggest far from the road, while immediately over the carriageway it is insignificant.

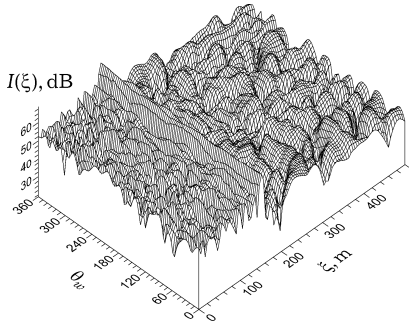

Fig. 7. Sound intensity distribution $I(\xi) = 20\log(|p_{tot}|/p_0)$ along bisector $0 \le \xi \le 500$ m, $\theta = 315°$ as a function of wind direction θ_w ($v_w = 40$ km/h) in the moment of time $t = 0$ s.

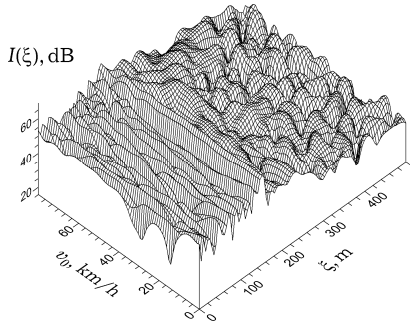

Fig. 8. Sound intensity distribution $I(\xi) = 20\log(|p_{tot}|/p_0)$ along bisector $0 \le \xi \le 500$ m, $\theta = 315°$ as a function vehicles velocity $v_0 = v_L = v_C$ ($v_w = 40$ km/h, $\theta_w = 315°$) in the moment of time $t = 0$ s.

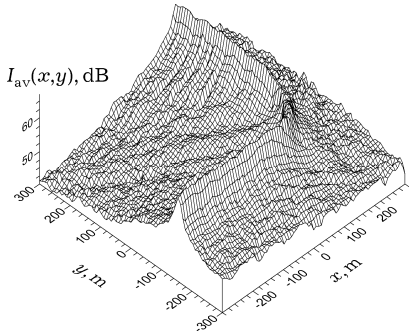

Fig. 9. Average sound intensity distribution in space $I_{av}(x, y)$ on the square 600×600 m^2, $z = 4$ m in windless conditions.

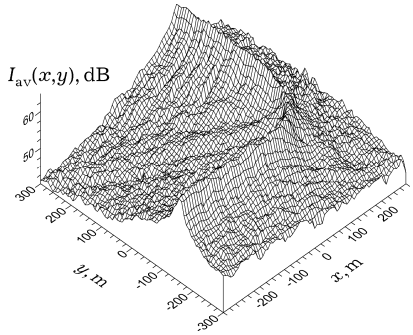

Fig. 10. Average sound intensity distribution in space $I_{av}(x, y)$ on the square 600×600 m^2, $z = 8$ m in windless conditions.

Figs. 9–11 show the distribution of acoustic sound intensity in space $I_{av}(\mathbf{x})$ averaged over time period $T_0 = 40$ s for $z = 4, 8$ and 12 m. In this case the calculations are obtained using (39) and (41) neglecting the effect of wind. It is shown that the right-angle bend in the road is the place of high noise concentration (near 66 dB), which decreases with an increase of the height and distance from this road section.

In Figs. 12–14, the distributions of sound intensity averaged power flow density $I_{av}(\mathbf{x})$ are displayed for $z = 4$ along bisector $0 \le \xi \le 500$ m, $\theta = 315°$ for different velocities v_w ($\theta_w = 315°$), directions θ_w ($v_w = 40$ km/h) and velocities v_0 ($v_w = 40$ km/h, $\theta_w = 315°$). These results have also shown that the effect of wind and motion of sound sources on sound intensity structure is the biggest far from the road.

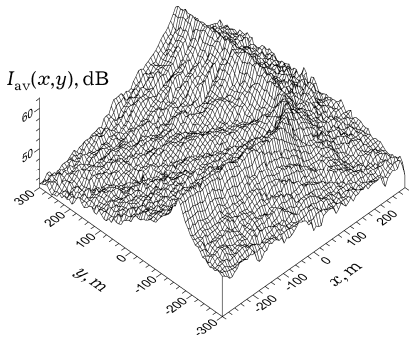

Fig. 11. Average sound intensity distribution in space $I_{av}(x,y)$ on the square 600×600 m^2, $z = 12$ m in windless conditions.

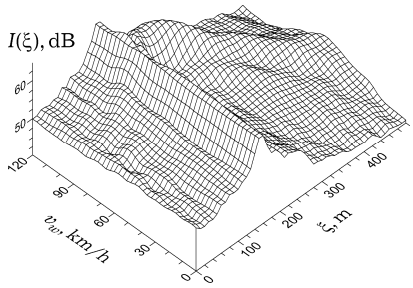

Fig. 12. Sound intensity distribution in space $I_{av}(x,y)$ averaged for time period 40 s along bisector $0 \le \xi \le 500$ m, $\theta = 315^\circ$ as a function of wind velocity v_w ($\theta_w = 315^\circ$, $v_0 = v_L = v_C = 40$ km/h).

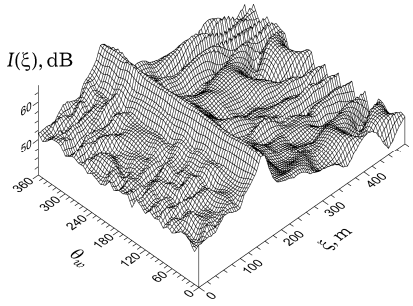

Fig. 13. Sound intensity distribution $I_{av}(\xi)$ averaged for time period 40 s along bisector $0 \le \xi \le 500$ m, $\theta = 315^\circ$ as a function of wind direction θ_w ($v_w = 40$ km/h, $v_0 = v_L = v_C = 40$ km/h).

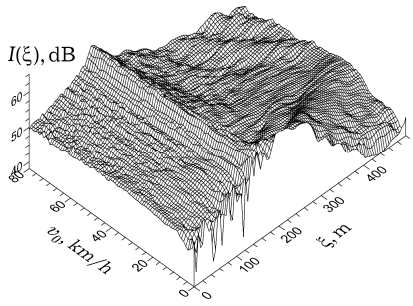

Fig. 14. Sound intensity distribution $I_{av}(\xi)$ averaged for time period 40 s along bisector $0 \le \xi \le 500$ m, $\theta = 315^\circ$ as a function of vehicles velocity $v_0 = v_L = v_C$ ($v_w = 40$ km/h, $\theta_w = 315^\circ$).

Conclusions. A new analytical approach to the description of vehicle sound radiation from a road bend taking into consideration wave reflection from the boundary interface: acoustic moving media – elastic solid half-space, is presented. A solution to this problem is obtained with the help of Fourier transforms over time and space variables in the plane parallel to the surface of elastic half-space. The same resulting integrals are calculated using the stationary phase method. The mathematical modeling was carried out for a dual carriageway road with three lanes each traveling in opposite directions of personal cars and heavy trucks. For numerical calculations data collected from one of Łódź streets were used. The analytical and numerical results of our work are as follows.

- The temporal structure of acoustic signal from a group of vehicles as the monopole sound sources moving on the road bend is very complicated and presented as a superposition of two series of quasi-sinusoidal pulses. The

calculations carried out in the immediate proximity to the road show that signals with bigger amplitudes (of the order of 0.05 Pa) belong to heavy transport, while signals with smaller amplitudes (of the order of 0.02 Pa, frequently) – to personal cars.

• The obtained formulas allow us to describe and estimate the acoustic field generated by vehicles traveling on the straight road sections and on the road bend. The straight and curved road sections are the places of high concentration of sound energy, where the acoustic pressure level can increase by $20 \div 30$ dB in comparison to the outside of road.

• The influence of wind and velocities of cars on the acoustical pressure and acoustical pressure level near road is important for the inner structure of these characteristics, but not for amplitude. The noise quickly weakens to the level of 50 dB with a small increase of the distance from the road axis and remains on this level in large space in the neighborhood of a road.

1. *Кеч В., Теодореску П.* Введение в теорию обобщенных функций с приложениями в технике. – Москва: Мир, 1978. – 518 с.
2. *Achenbach J. D.* Wave propagation in elastic solids. – Amsterdam: North-Holland Publ. Co.; New York: Amer. Elsevier Publ. Co., 1973. – xiv+425 p.
3. *Chevallier E., Leclercq L., Lelong J., Chatagnon R.* Dynamic noise modeling at roundabouts // Appl. Acoust. – 2009. – **70**, No. 5. – P. 761–770.
4. *Engel Z.* Ochrona środowiska przed drganiami i hałasem. – Warszawa: Państw. Wyd-wo Nauk., 2001. – 500 s. (in Polish).
5. *Felsen L. B., Marcuvitz N.* Radiation and scattering of waves. – Englewood Cliffs: Prentice-Hall Inc., 1973. – xxxiv+888 p.
6. *Kettil P., Engström G., Wiberg N.-E.* Coupled hydro-mechanical wave propagation in road structures // Comput. & Struct. – 2005. – **83**, No. 21-22. – P. 1719–1729.
7. *Morgan P. A., Nelson P. M., Steven H.* Integrated assessment of noise reduction measures in the road transport sector [TRL Limited/RWTÜV Fahrzeug GmbH]. – Project Report PR SE/652/03. – 2003. – 116 p.
8. *Morse P. M., Ingart K. U.* Theoretical acoustics. – New York: McGraw-Hill Book Co., 1968. – xxii+938 p.
9. *Piddubniak O., Piddubniak N.* Sound radiation from a roundabout // Arch. Acoust. – 2010. – **35**, No. 3. – P. 437–456.
10. *Piddubniak O., Piddubniak N., Kurek Ł., Dujka M.* Sound car radiation from city crossroad // In: DIPED–2009: Proc. XIVth Int. Seminar/Workshop on Direct and Inverse Problems of Electromagnetic and Acoustic Wave Theory, Lviv, Sept. 21–24, 2009. – Lviv, 2009. – P. 261–266.
11. *Piddubniak O., Piddubniak N., Mądra M.* Sound radiation from roadway with a right-angle winding // In: DIPED–2012: Proc. XVIIth Int. Seminar/Workshop on Direct and Inverse Problems of Electromagnetic and Acoustic Wave Theory, Tbilisi, Sept. 24–27, 2012. – Tbilisi, 2012. – P. 188–194.
12. *Piddubniak O., Piddubniak N., Teodorczyk T., Abramczyk J.* Radiation of roadway noise in windy conditions // In: DIPED–2009: Proc. XIVth Int. Seminar/Workshop on Direct and Inverse Problems of Electromagnetic and Acoustic Wave Theory, Lviv, Sept. 21–24, 2009. – Lviv, 2009. – P. 253–260.
13. *Rodríguez-Molares A., Sobreira-Seoane M. A., Martín-Herrero J.* Noise variability due to traffic spatial distribution // Appl. Acoust. – 2011. – **72**, No. 5. – P. 278–286.
14. *Tanaka S., Shiraishi B.* Wind effects on noise propagation for complicated geographical and road configurations // Appl. Acoust. – 2008. – **69**, No. 11. – P. 1038–1043.
15. *Wang L.* Mechanics of asphalt: Microstructure and micromechanics. – New York etc.: McGraw-Hill, 2011. – vi+474 p.
16. *Zhao J., Zhang X., Chen Y.* A novel traffic-noise prediction method for non-straight roads // Appl. Acoust. – 2012. – **73**, No. 3. – P. 276–280.

ВИПРОМІНЮВАННЯ ЗВУКУ АВТОМОБІЛЯМИ НА ПРЯМОКУТНОМУ ПОВОРОТІ ДОРОГИ

Вивчається задача звукового випромінювання автомобілями, які рухаються по міській вулиці з прямокутним поворотом. Враховується вплив вітру на акустичне поле. Спочатку розв'язок задачі одержано для двох точкових джерел шуму, які рухаються в протилежних напрямах, з використанням інтегральних перетворень Фур'є за просторовими змінними і часом. Обернені трансформанти обчислені наближено з використанням методу стаціонарної фази. Розв'язок загальної задачі одержано як суперпозицію багатьох часткових розв'язків. Числовий аналіз характеристик дорожнього шуму проведено для випадку вулиці Текстильників з двостороннім рухом в Лодзі, Польща.

ИЗЛУЧЕНИЕ ЗВУКА АВТОМОБИЛЯМИ НА ПРЯМОУГОЛЬНОМ ПОВОРОТЕ ДОРОГИ

Изучается задача звукового излучения автомобилями, двигающимися по городской улице с прямоугольным поворотом. Учитывается влияние ветра на акустическое поле. Сначала решение задачи получено для двух точечных источников шума, передвигающихся в противоположных направлениях, с использованием интегральных преобразований Фурье по пространственным переменным и времени. Обратные трансформанты определены приближенно с использованием метода стационарной фазы. Решение общей задачи получено в виде суперпозиции многих частных решений. Численный анализ характеристик дорожного шума проведен для случая улицы Текстильщиков с двусторонним движением в Лодзи, Польша.

Lodz Univ. of Technology, Lodz, Poland,
Lviv Polytechnic National Univ., Lviv

Received
10.08.15